

## RESEARCH ARTICLE

### Construction Engineering

# Thermal performance of glass facade under fire loading: a numerical approach

RGSS Perera, JHA Ruwanmali, T Thevega, JASC Jayasinghe\*, CS Bandara and AJ Dammika

*Department of Civil Engineering, Faculty of Engineering, University of Peradeniya, Peradeniya, Sri Lanka.*

Submitted: 28 June 2023; Revised: 01 December 2023; Accepted: 26 February 2024

**Abstract:** Non-structural internal and external walls play a crucial role in high-rise buildings. Exterior walls contribute to the building's aesthetic appearance and create a comfortable indoor environment against thermal and wind effects. Interior walls divide the space and minimize sound distractions while maintaining desired conditions. External walls are particularly important as the presence of combustible materials can pose a significant fire hazard. Hence, it is crucial to use materials with high thermal performance to mitigate risks. Glass is a commonly used material for external walls due to its transparency, affordability, availability, and sustainability. However, glass panels are susceptible to failure when exposed to heat due to their brittleness. Therefore, this study aims to assess the thermal performance of glass panels under fire by analyzing single, laminated, and insulated glass panels using *ABAQUS* finite element software. Through a parametric study using validated numerical models, the study identifies the optimal configuration for glass panels. The findings indicate that increasing the thickness of a single glass panel by 2 mm resulted in a temperature decrease of approximately 13.5%. Additionally, the impact of shape on thermal performance is studied by evaluating crack initiation time and temperature for various shapes with equal areas. The results show that rectangular panels exhibit the poorest thermal performance. Furthermore, the type of glass panel significantly influences thermal performance compared to shape and thickness. Insulated glass panels demonstrate superior performance compared to single and laminated glass panels. When investigating different insulation materials, krypton outperforms argon and air in terms of thermal performance. This study contributes to the advancement of fire-safety solutions in buildings by using a validated numerical model to identify critical parameters

affecting the thermal performance of glass facades across various types and configurations.

**Keywords:** Finite element analysis, glass facades, insulated glass panel, laminated glass panel, thermal loads.

## INTRODUCTION

There are two main types of building elements: structural and non-structural elements. Structural elements, including slabs, columns, beams, and foundations, are load-bearing and support the weight of the building. Non-structural elements, such as ceilings, windows, doors, and wall panels, do not bear the dead and live loads but should withstand the impact and environmental loads. This study focuses specifically on non-load-bearing wall panels, which are essential components in high-rise buildings. Wall panels can be categorized as either interior or exterior. Interior wall panels are used to partition the building into rooms and must be able to withstand fire, seismic load, and self-weight. Exterior wall panels, on the other hand, must be able to withstand wind, seismic load, fire, and self-weight. Additionally, they must enhance the building's exterior appearance and protect occupants from external loads such as wind and fire. Fire is considered one of the most devastating hazards that buildings and other structures can face (Kodur, 2014; SFPE series, 2022). Structural fire damage results in numerous fatalities, injuries, and millions in property damage worldwide on an annual basis (Brushlinsky

\* Corresponding author ([supunj@eng.pdn.ac.lk](mailto:supunj@eng.pdn.ac.lk);  <https://orcid.org/0000-0003-1054-9358>)



This article is published under the Creative Commons CC-BY-ND License (<http://creativecommons.org/licenses/by-nd/4.0/>). This license permits use, distribution and reproduction, commercial and non-commercial, provided that the original work is properly cited and is not changed in anyway.

*et al.*, 2007; Kodur *et al.*, 2020). According to data from the Centre of Fire Statistics (CTIF, 2018), approximately 510,000 structural fire incidents are reported each year, indicating that a structural fire occurs somewhere in the world every 62 seconds.

Wall panels can be manufactured in various shapes and sizes to meet different design requirements.

In modern construction, the most popular types of exterior wall panels include lightweight concrete precast sandwich panels, lightweight steel gauge framed panels, and curtain wall panels. According to Moutassem & Alamara (2021), lightweight concrete precast sandwich panels are typically composed of facing, core, and connector materials. The facing materials provide structural integrity and durability, while the core material provides fire resistance. Connectors are used to join the materials together (O'Hegarty & Kinnane, 2020). The advantages of these wall panels are that they are environmentally friendly, durable, fire and impact-resistant, economical, lightweight, and can be rapidly installed. However, the disadvantages include a lack of strength and more segregation (Fayez & Kadhim, 2021). Lightweight steel gauge framed (LSF) wall panels are made up of a steel frame, sheathing panel, cavity insulation, and an external thermal insulation composite (ETIC) system (Kesawan & Mahendran, 2017; Santos *et al.*, 2019). Steel studs have higher thermal conductivity, which increases the heat transfer speed even in a normal fire. Due to the increased heat transfer of steel studs, there is a thermal bridge effect. This effect caused a decrease in the thermal resistance of the wall panel. Thermal break strips can be used to mitigate this effect (Santos & Mateus, 2020). The advantages of these wall panels are that they are economical, lightweight, require less maintenance, and can be rapidly installed. However, the main disadvantage is that they have high thermal conductivity. Vacuum insulation panel (VIP) is good as an insulation material for both LSF and concrete precast sandwich panels (Rajanaygam *et al.*, 2021). Curtain walls typically consist of metal frames and infill materials (No *et al.*, 2008; Lu *et al.*, 2016; Oh *et al.*, 2016). Metals such as aluminium and steel can be used as frame materials. The infill materials play a crucial role in providing a modern and aesthetically pleasing appearance while protecting the occupants and reducing environmental impacts.

The mechanical performance of wall panels is typically considered during the design, but thermal performance is often overlooked. This has led to major fire incidents in buildings in the past, with wall panel types being the

primary factor for fire spread (Guillaume *et al.*, 2018). In recent times, curtain wall panels have become more popular due to their numerous advantages over other wall panel types. These panels can be categorized based on their infill material as either combustible or non-combustible. Non-combustible materials are preferable due to their lower fire-spreading risk in large panel areas (Bonner & Rein, 2018; Yuen *et al.*, 2021). Glass is frequently utilized as a non-combustible material in curtain walls because of its lightweight, transparent, and eco-friendly characteristics, along with its positive aspects in terms of daylighting and views. Nevertheless, glass is susceptible to sudden failure under thermal and mechanical stresses due to its high brittleness and weakness in tension. The non-flammable glass material is identified as weak under heat loadings (Shields *et al.*, 2001, 2002; Wang *et al.*, 2016; Wang *et al.*, 2018). Therefore, critical consideration of the breaking temperature of a glass facade and the impact parameters is essential, as beyond this point, the glass is incapable of bearing any load and necessitates replacement.

Glass can be classified based on the manufacturing process, including float annealed glass (AN), heat-strengthened glass (HS), and fully tempered glass (FT). AN glass is produced using the float manufacturing process (Nodehi, 2016), which offers the advantages of low cost, wide availability, good quality, and the ability to produce large panes of glass. It is the most economical but has lower strength compared to the other two types (Beton *et al.*, 2018). HS glass is produced by heating the float glass and cooling it at a lower rate. This glass is about two times stronger than AN glass because of residual surface compression resulting from thermal strain compatibility through the glass thickness during the heating and cooling processes (Beton *et al.*, 2018). FT glass is made by heating AN glass to above 700°C and then force-cooling it, providing substantially higher surface compression compared to HS glass. This makes FT glass four to five times stronger than AN glass, with very high tensile strength (Beton *et al.*, 2018).

Single, laminated, and insulated glass panels are popular choices for curtain wall panels at present. A single glass panel consists of a single glass plate. Glass plates are commonly fused together to create laminated glass components using interlayer polymers such as polyvinyl butyral (PVB) and Ethyl vinyl acetate (EVA) that generate adhesion forces during lamination (Santarsiero *et al.*, 2018). The inter-layer moderates the impact energy and modifies the brittle fracture (Vedrtam & Pawar, 2017). The designed fracture of laminated glass is contingent on the type of glass as well as the

type and thickness of interlayer used. Generally, the PVB interlayer is not fully bonded to the glass, and the impact resistance of the laminated glass plate is higher than that of a glass plate of the same thickness. However, the impact fracture behaviour of laminated glass is complicated due to the combined influence of large deformation and delamination strength. The brittle nature of glass, the nonlinear characteristics of PVB, and the adhesive bonding make the impact damage behaviours of laminated glass much more complicated (Keller *et al.*, 1999). Insulating glass is a building material that is used to reduce heat loss within a building. It consists of two or more glass panes and a gas-filled gap (Cuce, 2018). The gas within the gap acts as a barrier against heat and sound, with gases such as argon and krypton that are commonly used. However, according to Wang *et al.* (2017), this is better for insulation, but it is easily subjected to fire. The thermal performance of insulated glass panels mainly depends on the cavity thickness and cavity gas type (Erdem, 2018). This type of glass panel can significantly reduce air conditioning costs, noise penetration, and UV transmission.

Most researchers were concerned about the thermal performance of float glass with rectangular and square shapes. Wang analyzed the thermal performance of laminated and insulated glass with variations in cavity thickness and insulation material (Wang *et al.*, 2017, 2017a). As experimental tests are expensive, consume more time, and negatively affect the environment, numerical analysis is preferred for a large amount of analysis. Also, numerical modelling offers a cost-effective, flexible, and efficient approach to studying complex systems. Especially for parametric studies with a large number of parameters and repeated processes, developed numerical technology gives great support. In recent years, modelling heat transfer effects has become increasingly critical in product design, including fields such as electronics, automotive, and medical industries. By utilizing computer simulations, engineers and researchers can optimize process efficiency and explore new designs while also reducing the need for costly experimental trials.

The aim of this study is to evaluate the thermal performance of glass facades under fire loadings using numerical analysis. The thermal performances of single, laminated, and insulated glass panels are investigated numerically using *ABAQUS* finite element software. First, numerical models of these panels are validated based on past experimental results. Then parametric study is conducted on the thermal effects by varying the shape, thickness, and type of glass panels. This analysis

was done using float glass with thicknesses of 6 mm, 8 mm, and 10 mm and square, rectangular, and triangular shapes. The effect of heating on single glass panels is evaluated by measuring the temperature variation and breaking temperature when changing thickness and shape. After that, the thermal behaviour of laminated and insulated glass panels is obtained by measuring only the temperature variation when changing interlayer thickness and cavity thickness, respectively. Finally, the improvement in the thermal response of insulated glass panels is observed with different insulation materials such as air, argon, and krypton. These analyses give a clear overview of the usage of different types of glass panels in different geometric configurations under various conditions.

---

## MATERIALS AND METHODS

### Modelling methodology

The thermal analysis of the glass wall panel is numerically carried out in *ABAQUS* software using a past study (Wang *et al.*, 2017). *ABAQUS* is a commercially available finite element software capable of performing simple linear analysis of the most complex non-linear simulations, as described by the SIMULIA User Assistance (2021).

To model the behaviour of a single glass panel, a laminated glass panel, and an insulated glass panel, 3D deformable solid parts were created and partitioned into exposed and covered regions for heat analysis. Material data from Table 1 was assigned to the glass section, and a heat transfer step in the transient state was used to obtain temperature variation results from the non-heated side to the heat, as described by Wang *et al.* (2017). The modelling utilized initial and heat transfer boundary conditions. As shown in Figure 1, the ENCASTRE ( $U1 = U2 = U3 = UR1 = UR2 = UR3 = 0$ ) initial boundary condition was applied to the four partitioning edges of both the exposed and non-exposed surfaces as a fixed boundary condition. The heat transfer boundary condition was applied to the average temperature in the exposed and covered areas at each time obtained from experimental results. Heat can be transferred via conduction, convection, and radiation, all of which require a temperature difference and occur from high-temperature to low-temperature mediums. Conduction, convection, and radiation occurred through the glass, cavity gas, and exposed area, respectively, to the environment. The heat transfer step used an initial temperature of 280 K as a predefined field and the Stefan Boltzmann constant of  $5.67 \times 10^{-8} \text{ W/m}^2\text{K}^4$ . Figure 2(a) illustrates the geometry of a 6 mm thick, single-coated float glass panel.

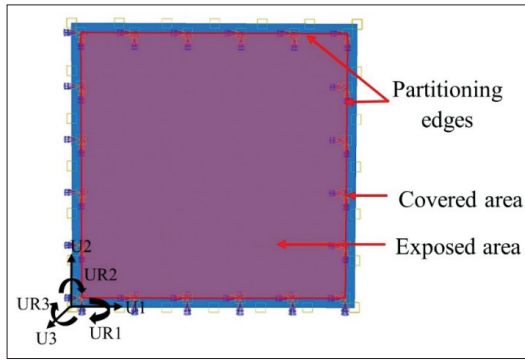


**Figure 1:** Assigned boundary conditions of the wall for numerical analysis

**Table 1:** Material properties (Wang *et al.*, 2017)

Properties	Symbol	Value
<b>Glass</b>		
Density (kg/m <sup>3</sup> )	$\rho$	2,500
Modulus of elasticity (Pa)	$E$	$7.3 \times 10^{10}$
Poisson ratio	$\nu$	0.17
Thermal expansion coefficient (1/K)	$\beta$	$8.46 \times 10^{-6}$
Reference temperature (K)	$T_R$	280
Specific heat capacity (J/(kg.K))	$C$	820
Thermal conductivity (W/(m.K))	$K$	0.94
Emissivity	$\epsilon$	0.85
<b>PVB</b>		
Density (kg/m <sup>3</sup> )	$\rho_{PVB}$	1,070
Specific heat capacity (J/(kg.K))	$C_{PVB}$	1,100
Thermal conductivity (W/(m.K))	$k_{PVB}$	0.221
<b>Air</b>		
Density (kg/m <sup>3</sup> )	$\rho_{air}$	1.16
Specific heat capacity (J/(kg.K))	$C_{air}$	1,007
Thermal conductivity (W/(m.K))	$k_{air}$	0.0263

In addition, as glass is a brittle material, the brittle crack model in *ABAQUS* software was used to investigate the breaking behaviour of the single glass panel. The material properties of the brittle cracking model can be found in Table 2 (Khan *et al.*, 2016). The dynamic analysis was used to obtain the breaking behaviour of the single glass panel in a temperature-displacement explicit step.

**Table 2:** Brittle material properties (Khan *et al.*, 2016)

	Direct stress after cracking (MPa)	Direct cracking strain
Brittle cracking	36.8	0
	34.1	0.000333
	21.1	0.000667
Direct cracking failure strain	$1 \times 10^{-6}$	
Brittle shear	Shear retention factor	Crack opening strain
	1	0
	0.5	0.001
	0.25	0.002
	0.125	0.003

Next to the single glass panel, the model for the laminated glass panel, consisting of two 6 mm single-coated float glass panels with a 0.38 mm interlayer of polyvinyl butyral (PVB) film, is depicted in Figure 2(b). The model for the insulated glass panel, as shown in Figure 2(c), was created using two 6 mm single-coated float glass panels and a 6 mm thick air cavity. In the numerical model, the air gap was assumed to be stagnant, and heat was transferred through the air via conduction. Despite the dominance of convection in facilitating higher heat transfer rates, the effective thermal conductivity for air was specifically used to analyze heat transfer through conduction. The effective thermal conductivity ( $K_{eff}$ ) of the air is calculated using equations from Cengel *et al.* (2012).

## RESULTS AND DISCUSSION

### Validation

Numerical models for single-coated float glass panels, laminated glass panels, and insulated glass panels were developed using past data from Wang *et al.* (2017), and the variation of temperature was validated with experimental results. Initially, the temperature variation model for the single glass panel was validated by obtaining temperature outputs on the exposed surface of the non-heated side, using a finite element analysis with a  $4 \times 4 \times 3$  mesh (size). Figure 3 illustrates a comparison between the numerical and experimental results of the single glass panel.

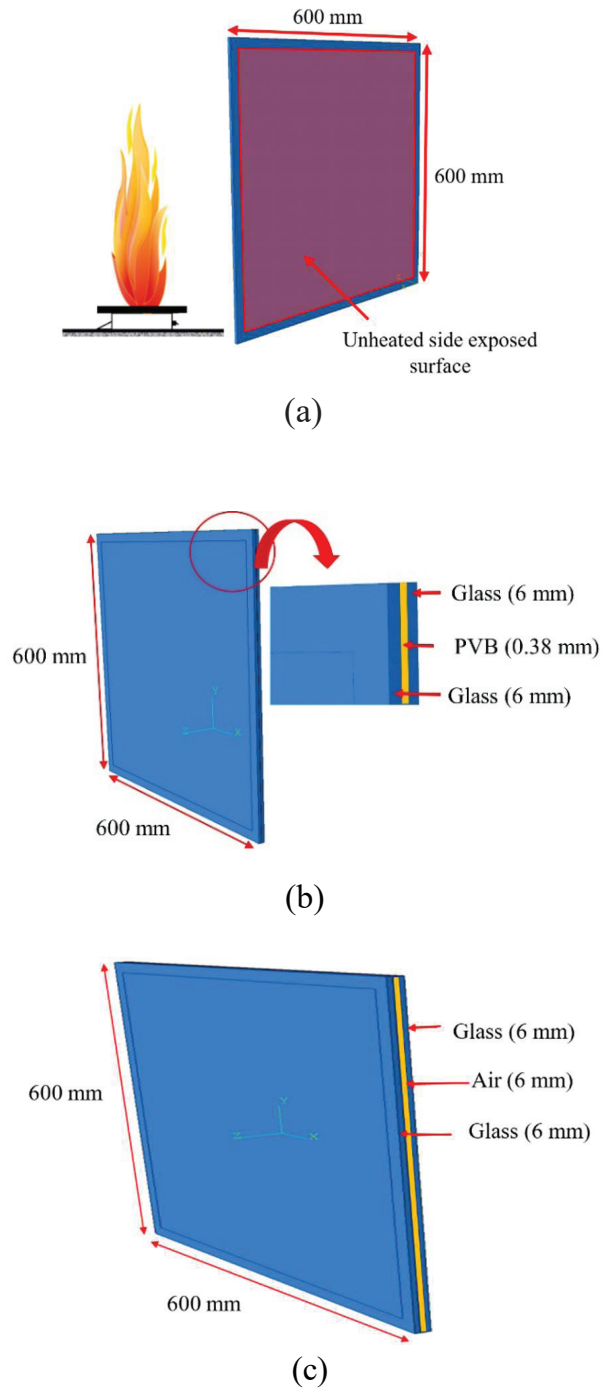


**Figure 2:** Geometric configuration of models: (a) Single; (b) Laminated, and (c) Insulated glass panel

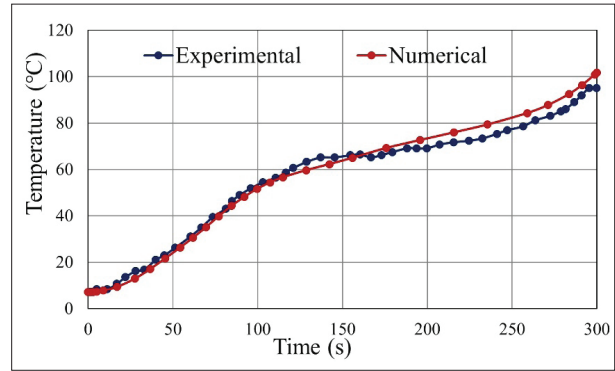


**Figure 3:** Comparison of experimental and numerical temperature variation results of single glass panel

The error between numerical and experimental results can be calculated by mean absolute deviation (MAD) as mentioned in equation 1. The MAD value for the single glass panel was calculated as 3.55, indicating a strong agreement between the experimental and numerical results. This suggests that the numerical model is reliable and can be used for further analysis and to investigate results.

$$MAD = \frac{\sum_{t=1}^n |y_t - \hat{y}|}{n} \quad \dots(01)$$

where  $y_t$  is the experimental temperature,  $\hat{y}$  is the numerical temperature, and  $n$  is the number of results.

The breaking temperature of the single glass panel was then analyzed. According to the experimental results of Wang *et al.*, (2017), numerical results of heat exposed side are investigated as the crack firstly occurs on the side of the glass panel to which heat is applied. As shown in Figure 4, cracks are initiated at the four corners of the heated side exposed area. When comparing the experimental and numerical results using absolute percentage error, the value was found to be 4.53%, indicating good agreement between both results. However, predicting the time of glass breakage remains a challenging task, as it is highly unpredictable. Experimental research is a useful approach to examining this issue, as suggested by Wang *et al.* (2014). Figure 5 shows the variation of maximum principal stress at the node where the crack was initiated (one corner).

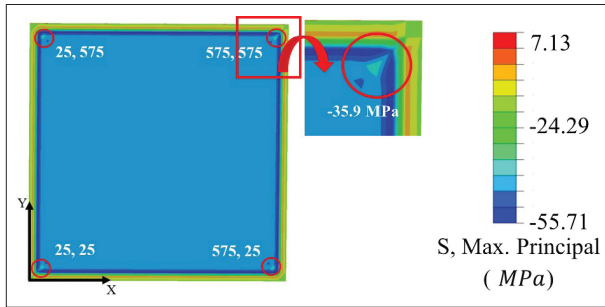


**Figure 4:** Variation of maximum principal stress and crack initiation points

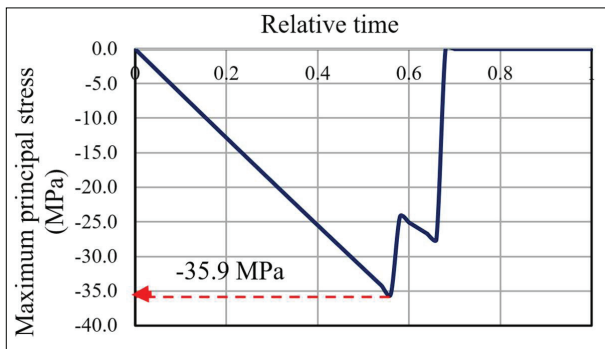


**Figure 5:** Variation of maximum principal stress at crack initiation node (at one corner)

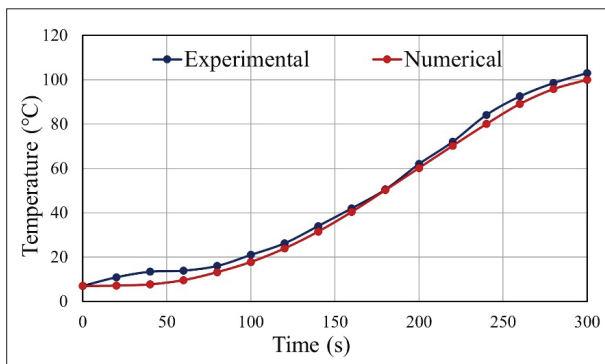


**Figure 6:** Comparison of experimental and numerical temperature variation results of laminated glass panel

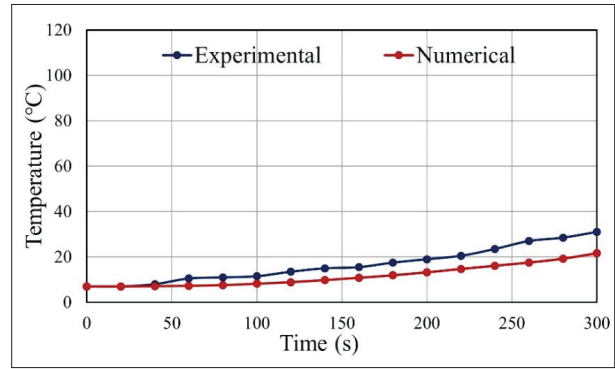


**Figure 7:** Comparison of experimental and numerical temperature variation results of insulated glass panel

After analyzing the thermal performance of a single panel, the temperature variations of the laminated glass panel and insulated glass panel were evaluated, and the results are shown in Figure 6 and Figure 7, respectively. The deviation between the experimental and numerical temperature values on the non-heated side of the exposed surface of the laminated glass is less than 3%, indicating good agreement between the two sets of data. The insulated glass model was created using air as cavity gas, assuming stagnancy. Based on Cengel *et al.* (2012), the effective thermal conductivity of air was calculated to reduce the effect of the stagnancy assumption. The MAD value for the insulated glass panel is 4.11, which can be expected due to the assumption of stagnant air.

**Parametric study of the glass panel**

The effect of different parameters, namely shape, thickness, and type, on the thermal performance of glass facades is analyzed while heating. The temperature variation of a single glass panel was investigated by changing the thickness with the same shape, and the breaking temperature was evaluated by changing the shape with the same cross-sectional area and the same thickness of glass panels. The thermal performance of square, rectangular, and triangular glass shapes with 6 mm, 8 mm, and 10 mm thicknesses were analyzed under fixed boundary conditions, as shown in Table 3. The effect on temperature variation was also studied for laminated glass panels with varying polyvinyl butyral

(PVB) film thicknesses of 0.38 mm, 0.76 mm, 1.14 mm, and 1.52 mm (Wang & Hu, 2019), as well as for insulated glass panels with varying cavity gas thicknesses of 8 mm, 16 mm, 24 mm, and 32 mm. Table 4 presents all the parametric study models of laminated and insulated glass panels. Finally, the variation of temperature for different glass panels, such as single, laminated, and insulated glass panels, was performed while considering the same volume of glass material.

**Table 3:** Models of a single glass panel

Shape	Thickness (mm)	Investigation factor
Square	6	Temperature variation
Square	8	
Square	10	
Square	8	Crack behaviour
Rectangular	8	
Triangular	8	

**Table 4:** Models of laminated and insulated glass panels

Glass type	PVB film / cavity thickness (mm)
Laminated	0.38
	0.76
	1.14
	1.52
Insulated	8
	16
	24
	32

**Effects of thickness of glass**

The temperature variation of a square-shaped single glass panel was investigated with varying thickness, as shown in Figure 8. Figure 9 presents the non-heated side exposed area temperature values for different thicknesses at 300 seconds. It is noticeable that increasing the thickness of the single glass panel by 2 mm results in a temperature drop of approximately 13.5%, indicating a linear variation.

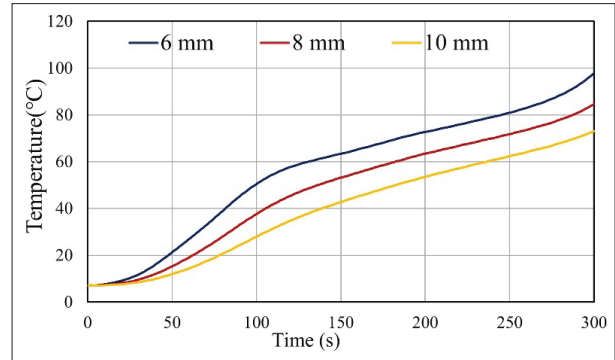


**Figure 8:** Comparison of temperature variation with glass thickness

Increasing the thickness of a glass panel makes it better at controlling temperature, as thicker glass provides improved insulation by resisting heat transfer more effectively. However, this comes with the major drawback of increasing the weight of the wall panel. To address this issue, an effective glass thickness of 8 mm was selected for further studies. Additionally, an increase in thickness leads to higher breaking stress and breaking time (Xie *et al.*, 2011). To investigate the breaking temperature, the

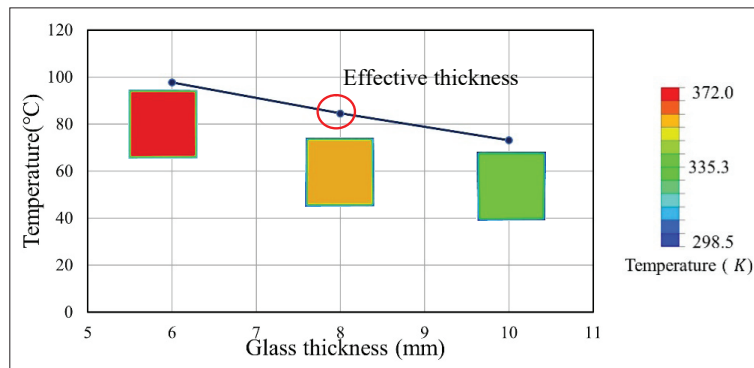


**Figure 9:** Comparison of the exposed surface of the non-heated side temperature values with glass thickness at 300 s

thickness was kept constant at 8 mm, and the thermal performance was analyzed by varying only the shape.

**Effects of the shape of the glass**

In Table 5, the breaking temperature and time of a single glass panel with an 8 mm thickness were analyzed under fixed boundary conditions while varying the shape. The volume of the glass panel was kept constant to maintain the constant weight of the glass panel. Aspect ratios

for rectangular and triangular shapes are 1 and 2.25, respectively. As observed in the experimental results, fracture is firstly observed at the corners of each shape due to the constraint stresses. The breaking behaviour results indicate that the rectangular shape is the worst shape for thermal performance. Due to the impact of the symmetric restraint condition on stress distribution, the square-shaped panel demonstrates enhanced performance in comparison to both rectangular and triangular panels.

**Table 5:** Maximum principal stress variation at crack initiate time

Shape of the glass panel (mm)	Breaking temperature (K)	Breaking time (s)
<p>Rectangular</p>	375.00	212.5
<p>Triangular</p>	378.66	228.1
<p>Square</p>	392.25	265.6

**Effects of type of glass**

The thickness of the glass greatly affects the thermal performance of a single glass panel. While increasing the thickness can enhance the performance significantly, it is not necessarily the optimum solution for the construction industry. Therefore, alternative methods must be explored to enhance the thermal performance of single-glass facades. In this regard, the temperature variation of the non-heated side exposed area of a square-shaped fixed-supported laminated glass panel was investigated by varying the PVB thickness, as shown in Figure 10. The laminated glass panel comprised two 8mm thickness single glass panels and a PVB layer. Figure 11 shows that the temperature drop between 0.38 mm and 0.76 mm

PVB thickness is 8.83%, while between 0.76 mm and 1.14 mm PVB thickness, it is 13.74%, and between 1.14 mm and 1.52 mm PVB thickness, it is 2.74%. While a greater thickness in the insulation material enhances heat resistance, improvements become less significant beyond a certain point. Therefore, the suggested optimal solution, considering both cost and total weight, is the laminated glass panel with a 1.14 mm PVB thickness.

Figure 12 shows the temperature variation at the exposed surface of the non-heated side of the insulated glass panel with an 8 mm thickness of each single glass panel by creating cavity thicknesses of 8 mm, 16 mm, 24 mm, and 32 mm. Here, krypton is used as the cavity gas in the insulated glass panel. As depicted in Figure 13, the temperature drop between an 8 mm and 16 mm cavity thickness is 14.67%, between a 16 mm and 24 mm cavity thickness is 5.62%, and between a 24 mm and 32 mm cavity thickness is 3.20%. It is evident that as the cavity thickness increases, the transferring rate of temperature decreases, but the volume of gas increases, leading to an increase in the total weight (weight increase is negligible if it is only glass) and the cost of the glass panel. As per the technical code for glass curtain wall engineering, 2003, the cavity thickness is typically between 12 mm to 20 mm. Within this range, the thickness does substantially impact the insulating properties, with smaller cavity thickness having greater heat conduction through the cavity gas, and larger gaps allowing more convection within the space, leading to higher convective heat loss. As such, a 16 mm cavity thickness is often selected as the optimum thickness for insulated glass panels.

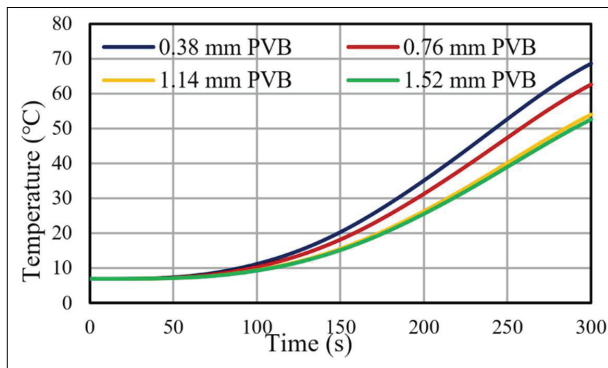


**Figure 10:** The variation of temperature with time for different PVB thicknesses of laminated glass panels

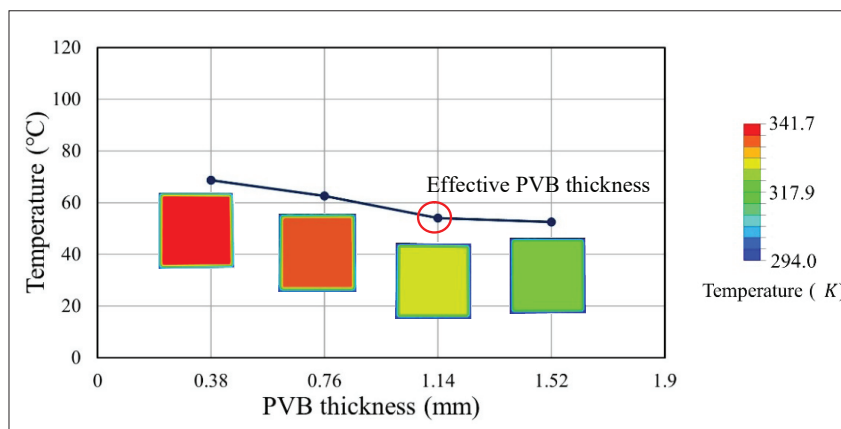


**Figure 11:** Comparison of the exposed surface of the non-heated side temperature values with different PVB thicknesses of laminated glass panels at 300 s

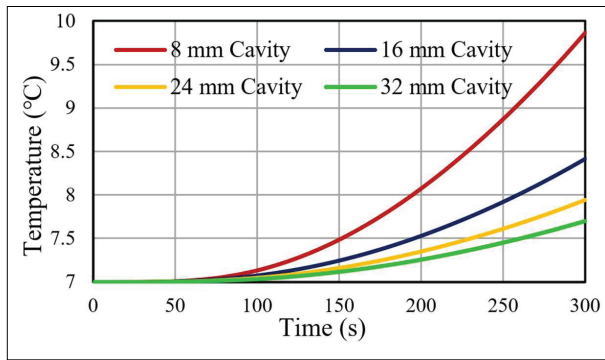


**Figure 12:** The variation of temperature with time for different cavity thicknesses of insulated glass panels (the cavity is filled with krypton)

To compare the effect of different types of glass panels, single, laminated and insulated glass panels were selected with the same weight of glass material. A 16 mm single glass panel, a laminated glass panel with two 8 mm glass panels and 1.14 mm PVB thickness, and an insulated glass panel with two 8 mm glass panels and 16 mm cavity thickness were modelled and analyzed under the same thermal loading, as shown in Figure 14. The variation of exposed surface temperature at the non-heated side with time for different glass panels is shown in Figure 15. At 300 seconds, the temperature drops between the single glass panel and the laminated glass panel (1.14 mm PVB thickness) is 28.13%, and between the single glass panel and the insulated glass panel (16 mm cavity thickness) is 81.51%. Hence, the order of the temperature increase rate on the non-heated

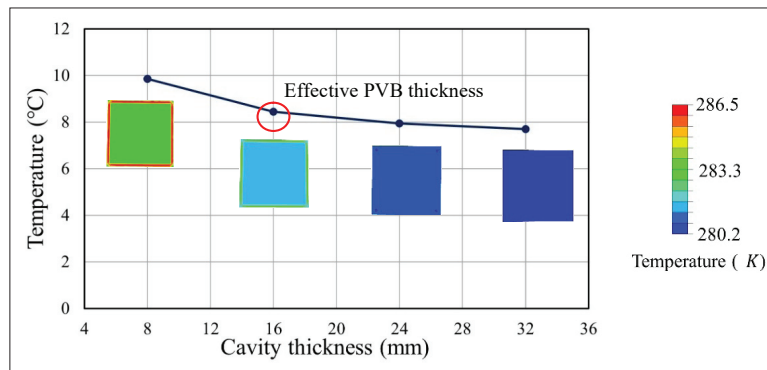


**Figure 13:** Comparison temperature with cavity thickness of insulated glass panel at 300 s (krypton)

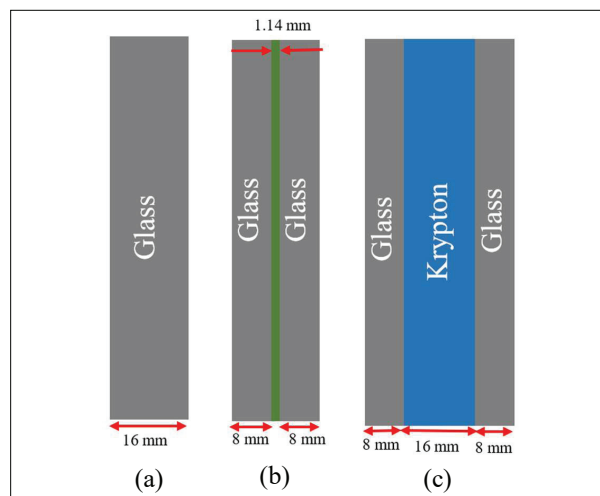


**Figure 14:** Geometric arrangement: (a) single; (b) laminated, and (c) insulated glass panels

side exposed surface is as follows: single > laminated > insulated. Among them, as the conductivity of gas is less than the solid material, the heat transfer in the insulated panel is less than the laminated panel. Figure 16 displays

the temperature variation along the thickness of the glass panels at 300 seconds. Owing to the symmetry of temperature variation, Figure 16 depicts the top half of the wall panel.

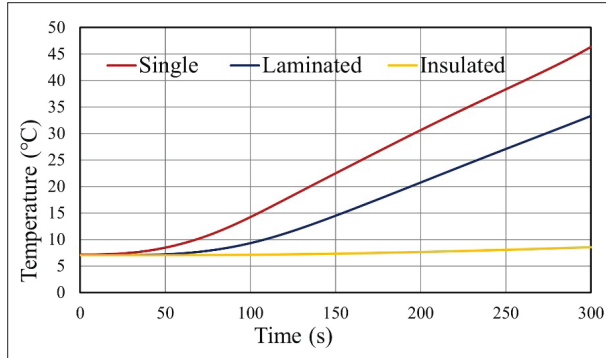


Figure 15: Comparison of temperature variation with different glass panels

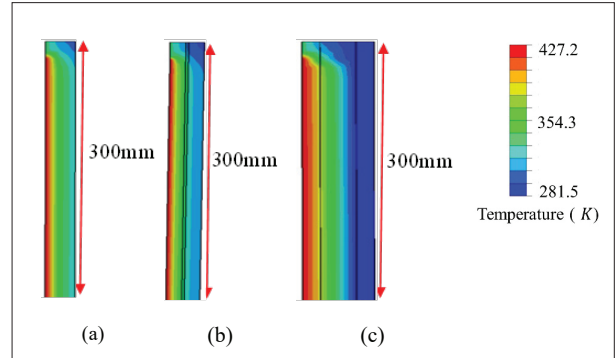


Figure 16: Comparison of temperature variation with different glass panels along thickness at 300 s: (a) Single; (b) Laminated, and (c) Insulated glass panels

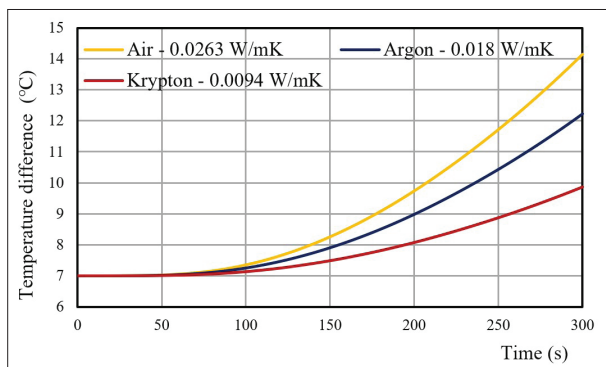


Figure 17: Comparison of temperature variation with different insulation materials of insulated glass panel

### Insulated glass panel with different insulation materials

The thermal performance of these insulated glass panels mainly depends on the cavity thickness and the cavity gas type (Cuce, 2018). In this study, three different cavity gases, namely air, argon, and krypton, were investigated to determine their impact on the thermal performance of square-shaped insulated glass panels with fixed support. The glass panels consisted of two 8 mm single glass panels with an 8 mm cavity. The thermal conductivity of the glass panel plays a critical role in determining its thermal performance. Materials with lower thermal

conductivity tend to have better thermal performance since they conduct less heat energy (Buck & Rudtsch, 2006). Krypton, with a thermal conductivity of 0.0094 W/m.K (Kralj *et al.*, 2011), has a lower thermal conductivity than both air and argon, resulting in better thermal performance than the other two gases. Figure 17 shows a comparison of temperature variation results on the non-heated side exposed area with varying insulation materials.

### CONCLUSION

In this study, numerical analysis was carried out to evaluate the thermal performance of float glass facades of different types and different geometric configurations under fire loadings using *ABAQUS* software. The study investigated the temperature variation on the non-heated side of single, laminated, and insulated glass panels. Furthermore, the study examined the temperature and time at which cracks were initiated in single glass panels. Based on the findings, the following conclusions are drawn:

- As experimental tests are not supportive of all the analyses, the thermal performance of glass facades can be investigated by analyzing the heat-transferring process using finite element numerical simulations.
- In single glass panels, surface temperature varies with thickness; it is reduced by around 13.5% when increasing the thickness by 2 mm. The crack-initiating temperature and crack-initiating time depend on the

shape of the glass, and the worst shape for the given fixed boundary condition is a rectangular shape (Aspect ratios for rectangular and triangular shapes were used 1 and 2.25, respectively).

- The laminated glass panel analysis proved that increasing the PVB layer thickness can further reduce temperature. Specifically, at 300 seconds, the temperature drop between PVB thickness of 0.38 mm and 0.76 mm is 8.83%, while the temperature drop between 0.76 mm and 1.14 mm is 13.74%. Additionally, the temperature drop between 1.14 mm and 1.52 mm is 2.74%.
- The non-heated side temperature of the insulated glass panel can be reduced by increasing the cavity thickness. Specifically, at 300 seconds, the temperature drop between 8 mm and 16 mm cavity thickness is 14.67%, while the temperature drop between 16 mm and 24 mm is 5.62%. Furthermore, the temperature drop between 24 mm and 32 mm thickness is 3.20%.
- From the study of different glass panels at 300 seconds, the temperature drop between single and laminated glass panels is 36.15%, and between single and insulated glass panels is 90.04%. As a result, the order of the temperature increase rate on the non-heated side exposed surface is single > laminated > insulated.
- According to the insulated glass model results, it can be concluded that at 300 seconds, the temperature drop between air and krypton is 30.32%, while the temperature drop between air and argon is 13.75%. Therefore, krypton is a more effective insulator than both air and argon.

## REFERENCES

- Bedon C., Zhang X., Santos F., Honfi D., Kozłowski M., Arrigoni M., Figuli L. & Lange D. (2018). Performance of structural glass facades under extreme loads - Design methods, existing research, current issues and trends. *Construction and Building Materials* **163**: 921–937.  
DOI: <https://doi.org/10.1016/j.conbuildmat.2017.12.153>
- Bonner M. & Rein G. (2018). Flammability and multi-objective performance of building facades: Towards optimum design. *International Journal of High-Rise Buildings* **7**(4): 363–374.  
DOI: <https://doi.org/10.21022/IJHRB.2018.7.4.363>
- Brushlinsky N., Ahrens M., Sokolov S. & Wagner P. (2007). *World Fire Statistics*. International Association of Fire and Rescue Services.
- Buck W. & Rudtsch S. (2006). Thermal properties. In: *Springer Handbook of Materials Measurement Methods* (eds H. Czichos, T. Saito & L. Smith). Springer Handbooks. Springer, Berlin, Heidelberg.
- Cengel Y.A., Cimbala J.M. & Turner R.H. (2012). *Fundamentals of Thermal fluid sciences*, chapter 19 & 20. McGraw Hill.
- CTIF. (2018). *World Fire Statistics*. Center for Fire Statistics of CTIF.
- Cuce E. (2018). Accurate and reliable U-value assessment of argon-filled double-glazed windows: A numerical and experimental investigation. *Energy and Buildings* **171**: 100–106.  
DOI: <https://doi.org/10.1016/j.enbuild.2018.04.036>
- Guillaume E., Fateh T., Schillinger R., Chiva R. & Ukleja S. (2018). Study of fire behaviour of facade mock-ups equipped with aluminium composite material-based claddings, using intermediate-scale test method. *Fire and Materials* **42**(5): 561–577.  
DOI: <https://doi.org/10.1002/fam.2635>
- Keller U. & Mortelmans H. (1999). June. Adhesion in laminated safety glass – what makes it work. *Glass Processing Days* **8**: 353–356.
- Keshawan S. & Mahendran M.A. (2017). Review of parameters influencing the fire performance of light gauge steel frame walls. *Fire Technology* **54**: 3–35.  
DOI: <https://doi.org/10.1007/s10694-017-0669-8>
- Khan A.J., Iqbal N., Saeed H.A. & Tarar W.A. (2016). Development of material model for assessment of brittle cracking behavior of plexiglas. *IOP Conference Series: Materials Science and Engineering* **146**(1).  
DOI: <https://doi.org/10.1088/1757-899X/146/1/012008>
- Kodur V. (2014). Properties of concrete at elevated temperatures. *ISRN Civil Engineering* **2**: 1–15.  
DOI: <https://doi.org/10.1155/2014/468510>
- Kodur V., Kumar P. & Rafi M.M. (2020). Fire hazard in buildings: review, assessment and strategies for improving fire safety. *PSU Research Review* **4**(1): 1–23.
- Kralj A., Znidarsic M., Fir M.J. & Remec C. (2011). Gas-filled panels as a high insulation alternative for 21<sup>st</sup> century building envelopes. *World Engineers' Convention*: 9.
- Lu W., Huang B., Mosalam K.M. & Chen S. (2016). Experimental evaluation of a glass curtain wall of a tall building. *Earthquake Engineering & Structural Dynamics* **45**: 1185–1205.
- Moutassem F. & Alamara K. (2021). Design and production of sustainable lightweight concrete precast sandwich panels for non-load bearing partition walls. *Cogent Engineering* **8**(1): 1–15.  
DOI: <https://doi.org/10.1080/23311916.2021.1993565>
- No S., Kim K. & Jung J. (2008). Simulation and mock-up tests of the thermal performance of curtain walls. *Energy and Buildings* **40**: 1135–1144.  
DOI: <http://doi:10.1016/j.enbuild.2007.10.004>
- Nodehi Z. (2016). Behaviour of structural glass at high temperatures. *Masters thesis*, Delft University of Technology, Netherlands.
- Oh J.H., Yoo H.J. & Kim S.S. (2016). Evaluation of strategies to improve the thermal performance of steel frames in curtain wall systems. *Energies* **9**(12): 1055.  
DOI: <https://doi.org/10.3390/en9121055>

- O'Hegarty R. & Kinnane O. (2020). Review of precast concrete sandwich panels and their innovations. *Construction and Building Materials* **233**: 117145.  
DOI: <https://doi.org/10.1016/j.conbuildmat.2019.117145>
- Rajanayagam H., Upasiri I., Poologanathan K., Gatheeshgar P., Sherlock P., Konthesingha C., Nagaratnam B. & Perera D. (2021). Thermal performance of LSF wall systems with vacuum insulation panels. *Buildings* **11**(12): 621.  
DOI: <https://doi.org/10.3390/buildings11120621>
- Santarsiero M., Bedon C. & Louter C. (2018). Experimental and numerical analysis of thick embedded laminated glass connections. *Composite Structures* **188**: 242–256.  
DOI: <https://doi.org/10.1016/j.compstruct.2018.01.002>
- Santos P., Lemes G. & Mateus D. (2019). Thermal transmittance of internal partition and external facade LSF walls: a parametric study. *Energies* **12**(14): 2671.  
DOI: <https://doi.org/10.3390/en12142671>
- Santos P. & Mateus D. (2020). Experimental assessment of thermal break strips performance in load-bearing and non-load bearing LSF walls. *Journal of Building Engineering* **32**: 101693.  
DOI: <https://doi.org/10.1016/j.jobe.2020.101693>
- Shields T.J., Silcock G.W.H. & Flood M.F. (2001). Performance of a single glazing assembly exposed to enclosure corner fires of increasing severity. *Fire and Materials* **25**: 123–152.  
DOI: <https://doi.org/10.1002/fam.764>
- Shields T.J., Silcock G.W.H. & Flood M.F. (2005). Behaviour of double glazing in corner Fires *Fire Technology* **41**: 37–65.
- SIMULIA User Assistance (2021). SFPE series (2022). *Fire Safety for Very Tall Buildings*. Springer.
- China Architecture & Building Press (2003). *Technical Code for Glass Curtain Wall Engineering*. Ministry of Construction of the People's Republic of China.
- Vedrtnam A. & Pawar S.J. (2017). Laminated plate theories and fracture of laminated glass plate A review. *Engineering Fracture Mechanics* **186**: 316–330.  
DOI: <https://doi.org/10.1016/j.engfracmech.2017.10.020>
- Wang Y. & Hu J. (2019). Performance of laminated glazing under fire conditions. *Composite Structures* **223**: 110903.  
DOI: <https://doi.org/10.1016/j.compstruct.2019.110903>
- Wang Y., Wang Q., Shao G., Chen H., Su Y., Sun J., He L. & Liew K.M. (2014). Fracture behavior of a four-point fixed glass curtain wall under fire conditions. *Fire Safety Journal* **67**: 24–34.  
DOI: <https://doi.org/10.1016/j.firesaf.2014.05.002>
- Wang Y., Wang Q., Sun J., He L. & Liew K.M. (2016). Influence of fire location on the thermal performance of glass façades. *Applied Thermal Engineering* **106**: 438–442.  
DOI: <http://dx.doi.org/10.1016/j.applthermaleng.2016.06.057>
- Wang Y., Wang Q., Wen J.X., Sun J. & Liew K.M. (2017). Investigation of thermal breakage and heat transfer in single, insulated and laminated glazing under fire conditions. *Applied Thermal Engineering* **125**: 662–672.  
DOI: <https://doi.org/10.1016/j.applthermaleng.2017.07.019>
- Wang Y., Wang Q., Su Y., Sun J., He L., and Liew K.M. (2017a). Experimental study on fire response of double-glazed panels in curtain walls. *Fire Safety Journal* **92**: 53–63.  
DOI: <https://doi.org/10.1016/j.firesaf.2017.05.016>
- Wang Y., Zhang Y., Wang Q., Yang Y. & Sun J. (2018). The effect of glass panel dimension on the fire response of glass façades. *Construction and Building Materials* **181**: 588–597.  
DOI: <https://doi.org/10.1016/j.conbuildmat.2018.06.088>
- Xie Q., Zhang H. & Si D. (2011). Experimental study on critical breakage stress of float glass with different thicknesses under conditions with temperatures of 25 and 200 C. *Fire and Materials* **35**(5): 275–283.  
DOI: <https://doi.org/10.1002/fam.1052>
- Yuen A.C.Y., Chen T.B.Y., Li A., De Cachinho Cordeiro I.M., Liu L., Liu H., Lo A.L.P., Chan Q.N. & Yeoh G.H. (2021). Evaluating the fire risk associated with cladding panels: An overview of fire incidents, policies, and future perspective in fire standards. *Fire and Materials* **45**(5): 663–689.  
DOI: <https://doi.org/10.1002/fam.2973>